Visible light-induced photopolymerization of Deep Eutectic Monomers, based on methacrylic acid and tetrabutylammonium salts with different anion structures

Samuel Wierzbicki [a], Kacper Mielczarek [a], Monika Topa-Skwarczyńska [a], Krystian Mokrzyński [b], Joanna Ortyl [a], Szczepan Bednarz [a,*]

[a] *Department of Biotechnology and Physical Chemistry, Cracow University of Technology, Warszawska 24, 31-155 Cracow, Poland*
[b] *Department of Biophysics, Faculty of Biochemistry, Biophysics and Biotechnology, Jagiellonian University, Gronostajowa 7, 30-387 Cracow, Poland*

ABSTRACT

Deep Eutectic Monomers were prepared by dissolution of selected tetrabutylammonium salts serving as hydrogen bond acceptors (HBA) in methacrylic acid (MAA) acting both as hydrogen bond donor (HBD) and vinyl monomer. In this study, we systematically investigate the influence of chloride, nitrate, hydrogensulphate and fluoroborate anions on properties of DEMs and the course of radical photopolymerization. By Combining FTIR, ^1H and ^{13}C NMR spectroscopy we found the that degree of coordination of MAA in DEMs by anions follows the order: $Cl^- > NO_3^- > HSO_4^- \gg BF_4^-$. Moreover, the studies indicated that the strength of hydrogen bonds between HBD and HBA in DEMs is lower than in MAA dimers. Real-time FT-IR spectroscopy studies of photopolymerization of DEMs indicate that the mixtures formed from MAA and tetrabutylammonium fluoroborate show significant lower initial photopolymerization rate in comparison with other investigated DEMs, which polymerize with similar rates.

1. Introduction

Deep eutectic solvents (DESs) belong to a class of ionic liquids (ILs). They are composed of low molecular weight organic compounds or inorganic salts. The lowering of the melting point is caused by strong intermolecular interactions between the constituents of the mixtures. The most common components of DESs are hydrogen bond donor (HBD) - hydrogen bond acceptor (HBA) pairs [1–3]. Analysis of the extensive research material indicates that quaternary ammonium chlorides (and in lesser extent bromides) are the most commonly used HBA, whereas carboxylic acids, amides, alcohols and phenols act as HBD. The literature also provides very new type of DESs composed of non-ionic components like menthol, thymol or camphor, called hydrofobic DES (ni-DES) around which interest has been growing [4]. In recent years ni-DESs were tested for many applications e.q extraction, metal removal from water or membranes [5–7].

From polymer chemistry perspective, also monomers could be components of DESs and serve both as HBD (e.g. acrylic, methacrylic, itaconic citric acids, resorcinol, glycerol) or as HBA (quaternary ammonium vinyl derivatives) [8]. To distinguish this subtype of DESs, the term Deep Eutectic Monomer (DEM) will be used in this work [9,10]. DEMs are new systems, not previously studied, and therefore the polymerization processes in such mixtures are poorly understood [8,11–13]. Interestingly, polymerized DEMs (PDEMs) have found many applications as solid electrolytes and flexible conductive materials, which deserves special attention, and is also a subject of many review articles [14–16]. Radical polymerization (RP) of DEMs can be initiated by thermal or photoinduced decomposition of the initiator as well as redox systems [9,17,18]. The great advantage of photoinitiation over the commonly used thermal initiation is the possibility to rapidly initiate polymerization at ambient temperature with low energy requirements and to shorten the duration of polymerization to few seconds [19]. The photopolymerization in DES was reported for the first time by Mecerreyes et al. [9,10]. The whole reaction was carried out with the use of a 2-cholinium bromide methacrylate monomer as an HBA and a variety of unreactive HBDs (e.g. citric acid, 1:1 M ratio HBA:HBD), which allowed achieving 100% monomer conversion (confirmed by ^1H NMR). Li et al. conducted photopolymerization of DEM based on acrylic acid and

* Corresponding author.
  E-mail address: sbednarz@pk.edu.pl (S. Bednarz).

choline chloride with a molar ratio of 1:1.6–2 obtaining 100% monomer conversion after 30 s of UV irradiation (confirmed by real-time FTIR). The PDEM thus obtained is a transparent and conductive elastomer [20]. The same research group also developed a rigid and self-healing material by photopolymerization of DEM consisting of choline chloride, acrylic acid and acrylamide with equal ratios of components [21]. Panzer et al. prepared a gel electrolyte by photoinduced RP of DES consisting of ethylene glycol, choline chloride and 2-hydroxyethyl methacrylate [22]. In turn, DES composed of bis(trifluoromethane)sulfonamide lithium salt and N-methylacetamide in a mixture with different monomers (2-hydroxyethyl acrylate, poly(ethylene glycol) methyl ether acrylate, 4- acryloylmorpholine and ethyleneglycol dimethacrylate) has been used by Logan et al. and Joos et al. to obtain gel electrolyte by photopolymerization [23,24].

Although photopolymerization has become a popular way to obtain PDEM materials, there has been only a few publications so far focused strictly on the kinetics of the photoinduced RP in DEMs. Pojman's research group used real-time FTIR spectroscopy to investigate the kinetics of the photopolymerization process in acrylic acid-choline chloride and methacrylic acid-choline chloride DEMs [25]. An increase of the polymerization rate for all the tested DES systems compared to those carried out in bulk was reported. The combined effect of DES's high viscosity, hydrogen bonding network and polarity was proposed as possible explanation. In another work, Li et al. investigated the copolymerization of acrylamide and acrylic acid both in bulk and in choline chloride:acrylic acid:acrylamide DEM by real-time FTIR. It has been shown that the copolymerization rate in analysed DEM is much faster than in bulk. What is more, in DES the monomer conversion reached almost 100% after 24 s, whereas in bulk polymerization it achieved only 15% after the same time of irradiation [21].

It is known that the anion structure determines the strength of hydrogen bonding in molecular complexes formed between HBA and HBD [26]. However, the influence of the anion structure of the quaternary ammonium salt (HBA) on the intermolecular interactions in DEM systems, and therefore the impact of this factor on the polymerization process of DEMs has not been investigated yet. Therefore, the purpose of the present work is to fill this gap and perform a systematic study on the influence of the anion structure of HBA on radical polymerization. In this work, we used tetrabutylammonium chloride, nitrate, hydrogensulphate and fluoroborate as HBDs and MAA as HBA. The spectroscopic properties of the DEMs were used for an explanation of the course of radical photopolymerization.

2. Experimental

2.1. Chemicals

Diphenyl(2,4,6-trimethylbenzoyl)phosphine oxide) (TPO, 97% purity), methacrylic acid (MAA, 99% purity containing 250 ppm of 4-methoxyphenol as inhibitor), quaternary ammonium salts (QX): tetrabutylammonium chloride (TBAC, 97% purity), tetrabutylammonium nitrate (TBANO, 97% purity), tetrabutylammonium hydrogensulfate (TBAHS, 97% purity) and tetrabutylammonium tetrafluoroborate (TBABF, 99% purity) were purchased from Sigma Aldrich and used without any further purification.

2.2. FTIR spectroscopy

The FTIR experiments were performed at room temperature on anIRSpirit FTIR (Shimadzu, Japan) spectrometer equipped with a crystal in horizontal attenuated total reflectance (ATR) cell. The spectral range was from 4000 to 450 cm^{-1}, the resolution was set to 2 cm^{-1}, and the spectra shown are an average of 32 scans.

The complex formation efficiency was defined as the ratio of heightsof the carbonyl stretching band of MAA-QX complex to the carbonyl stretching band of hydrogen-bonded dimers of MAA (B/A,

Fig. 2).

2.3. ^1H NMR and ^{13}C NMR spectroscopy

^1H NMR and ^{13}C NMR analysis were performed on a 500 MHz JOEL JNM-ECZR500 RS1 (JOEL Ltd., Japan) spectrometer. The DEM samples were loaded without solvent to a sealed NMR tube. Coaxial capillary with D$_2$O was inserted as an external reference. Because of high samples concentration, 8 scans for ^1H NMR analyses and 32 scans for ^{13}C NMR were sufficient to obtain spectra with high quality. Spectra were collected at 21 °C. The total sample measurement time (^1H and ^{13}C) was c.a. 5 min.

2.4. Density measurements

Density measurements were taken using a Kyoto KEM DA-640 (Kyoto Electronics Manufacturing CO., LTD., Japan) vibrating-tube densimeter. The instrument was calibrated at atmospheric pressure using ultrapure water and dry air. Measurements were carried out at atmospheric pressure at 25 °C (±0.05 °C), with the resolution of 1×10^{-4} g·cm^{-3}, and uncertainty of measurements of $\pm 5 \times 10^{-5}$ g·cm^{-3}.

2.5. Viscosity measurements

The viscosities were measured using an Anton Paar MCR 302 (Anton Paar, Austria) rheometer using a cone-plate CP50-1sensor. Measurements were conducted at 25 °C. The temperature was maintained using the integrated thermostat system. The viscosity was determined for the shear rate ranged from 30 to 100 s^{-1}.

2.6. RT-FTIR

The progress of free-radical photopolymerization of DEM was followed by real-time FT-IR spectroscopy using FT-IR i10 NICOLET^{TM} spectrometer equipped with a horizontal adapter (Thermo Scientific, USA). The evaluation of methacrylate group content was continuously followed at about 6164 cm^{-1}. Because the decrease of absorption of the peak area is directly proportional to the number of polymerized groups, conversion degree (X) of the functional group was by using Eq. (1):

$$X_{FT-IR}[\%] = \left(1 - \frac{A_t}{A_0}\right) \cdot 100\% \tag{1}$$

where:A$_0$ is an area of the absorbance peak of C=C vibration overtone before polymerization, and A$_t$ is an area of the peak at certain photopolymerization time. LED emitted the blue edge of the visible spectrum (emission maximum 405 nm, Thorlabs Inc., USA) with the insensitivity: 19.8 mW/cm^2, 1.0 mW/cm^2, and 0.2 mW/cm^2 was used to initiate the photopolymerization. The light source was switched on 10 s after the start of spectral acquisition. The distance between the LED and the reaction mixtures, which were placed in a 1.4 mm thick ring, was 2.1 cm. The initial concentration of the TPO photoinitiator was 2 mg/ml of the mixture. Additionally, during the photopolymerization process, the temperature of the samples was monitored using a thermal imaging camera from Dongguan Xintai Instrument Co., Ltd. (see Figs. S12 and S13).

2.7. Size excusion chromatography

Size exclusion chromatography (SEC) was carried out in phosphate buffer (0.1 M) at 40 °C using Knauer AZURA liquid chromatography system (KNAUER, Germany) with Knauer Azura RID 2.1L refractive index detector. Analyses were conducted using Phenomenex PolySep_GFC-P Linear column calibrated with poly(methacrylic acid) sodium salt standards.

2.8. Time – resolved EPR spectroscopy

The EPR measurements were run using a Bruker-EMX AA spectrometer (Bruker BioSpin, Germany) and a dedicated custom-made high-power 405 nm LED chip (light intensity of 13.1 mW/cm^{2}CHANZON, China). The first scan was obtained in the dark (LED OFF), then samples were irradiated for 6.75 s (LED ON), and after that the, decay of EPR signal was collected for 120 s in dark time (LED OFF). Samples of DEM with TPO photoinitiator (2 mg/ml) were placed in NMR tubes and located in the resonant cavity of EPR spectrometer. The following parameters were used for the EPR measurements: microwave power of 16.73 mW, modulation amplitude of 0.05 mT, centre field of 338.48 mT, sweep width of 2 mT and scan time of 3.375 s.

3. Results and discussion

3.1. Synthesis of DEMs

Preliminary studies have shown that variety of tetraalkylammonium salts with different cation and anion structures have very limited solubility in MAA and form at room temperature heterogeneous solid–liquid mixtures. However, we have found that some tetrabutylammonium salts (Fig. 1) are well soluble in MAA in a wide range of concentrations, what makes them useful in systematic studies. DEMs were prepared by heating the acid with the salt at selected molar ratios of HBD to HBA namely, 3:1, 4:1, 8:1 and 16:1 what corresponding to 75, 80, 88, 94 M % of MAA.

3.2. FTIR spectroscopy

In order to investigate the molecular HBD-HBA interactions, FTIR analyses were performed. Our studies focused on the analysis of the position, intensity and shape of carbonyl stretching band of MAA, because this vibration is sensitive to association state of carboxylic group [27,28]. Fig. 2 shows a schematic representation of the effect of H-bonding on the position of the carbonyl band on FTIR spectra.

Due to strong hydrogen bonding carboxylic acids exist as cyclic dimers and other higher-order associates. The carbonyl band corresponding to MAA dimers appears at 1690 cm^{-1}, whereas the vibration of the monomeric form of MAA shows absorption at higher wavenumbers [29]. Normalized FTIR spectra of carbonyl band region for DEMs composition are shown in Fig. 3. The demonstrated spectra reveal a decrease in the absorption intensity of the carbonyl band originating from the cyclic MAA dimer (1690 cm^{-1}) and a slight shift towards a higher wavenumber as the molar ratio of the HBA increases. In addition, one new band(Fig. 2, B) for TBAC (1708 cm^{-1}) , TBANO (1710 cm^{-1}) and TBABF (1719 cm^{-1}) and two extra bands for TBAHS(1676 cm^{-1} (C)
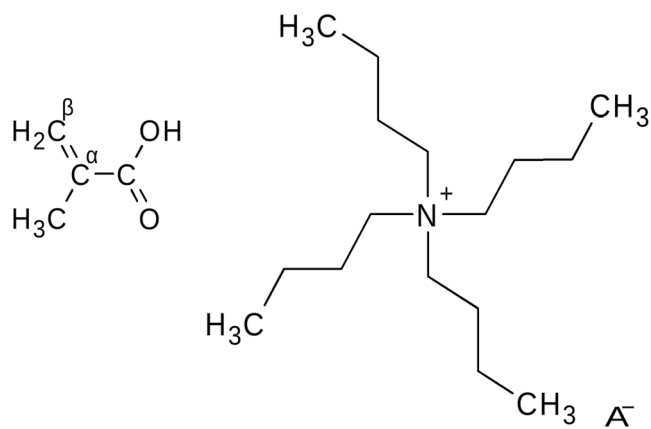

Fig. 1. Chemical structure of methacrylic acid and tetrabutylammonium salts used in this study. A$^-$: Cl$^-$ (TBAC), NO$_3^-$ (TBANO), HSO$_4^-$ (TBAHS) and BF$_4^-$ (TBABF).
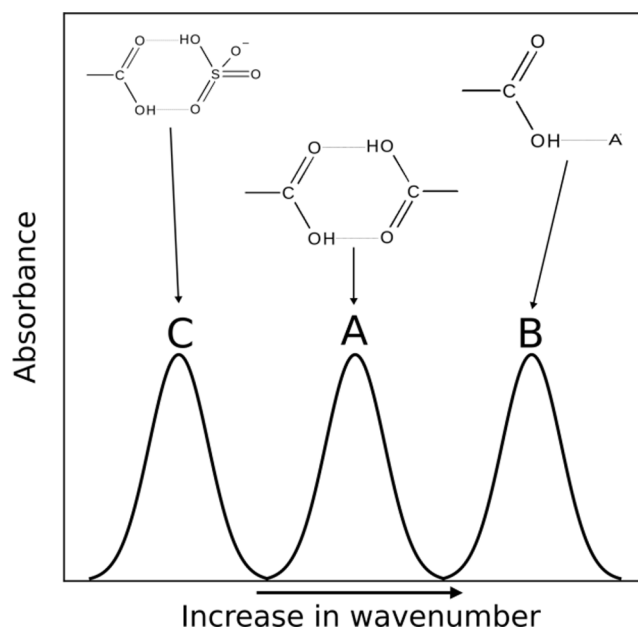

Fig. 2. Schematic representation of the effect of H-bonding on position of the carbonyl band vibration on FTIR spectra: (A) MAA dimers, (B) MAA-QX complex, (C) MAA-HSO$_4^-$ complex.

and 1713 cm^{-1}) appear. The new band appearing at higher wavenumbers (B) comes from MAA involved in complex formation with ammonium salts. This phenomenon have been reported before by Pojman and Mota-Morales for other carboxylic acid-based DES [30,31]. It can be concluded, that the interactions between MAA and anionic species leads to the breakdown of dimeric associates of MAA and formation of MAA-QX complexes.

The observed shift of carbonyl band toward higher wavenumbers in DEM indicates that the strength of hydrogen bonds in the MAA-QX complex is lower than in MAA dimers. In addition, the wavenumber of the carbonyl band of complexed MAA follows the order TBAC (1708 cm^{-1}) > TBANO (1710 cm^{-1}) > TBAHS (1713 cm^{-1}) > TBABF (1719 cm^{-1}), which may suggest that the H-bond energy between the carboxyl group of MAA and salt anions decreases according to the seriesCl$^-$ > NO$_3^-$ > HSO$_4^-$ > BF$_4^-$. The order perfect fits to the trend of H-bond acceptor parameters (β)determined for these anions using UV–VIS titration by molecular probes [26].

The second important feature is the intensity of the C=O band. The extent of the decrease in the C=O band intensity of cyclic dimers and increase in the C=O band intensity of complexed form indicates the efficiency of the formation of the monomer complexes by different anions (see Supplementary Materials Fig. S1). As can be seen in Fig. 2 the magnitudes of the changes in the spectra are strictly correlated with the H-bond energy between MAA and ammonium salts anions, due to the fact that higher H-bond energy increases competitiveness for the HBD group. The efficiency of monomeric complex formation by ammonium salts follows the same trend as the H-bond energy.

In the case of the MAA-TBAHS system, one extra vibration band at 1676 cm^{-1} is visible. Interactions between MAA and hydrogen sulphate anion can be interpreted similarly to a system composed of carboxylic acids and sulphuric acid in which the formation of cyclic complexes via two hydrogen bonds takes place [32]. One type of hydrogen bond is formed in a manner similar to the rest of the anions studied in this work, that is via carboxylic proton, and the second type of H-bond is formed by sharing of acidic proton in sulphuric anion (SO—H•••O=C—). It should be noted that carbonyl band corresponding to cyclic complexes MAA-TBAHS (1676 cm^{-1}) shows a greater red shift effect than carbonyl band MAA dimers (1696 cm^{-1}), which might indicate that SO—H•••O = C—H-bond has higher energy than CO—H•••O in acidic cyclic
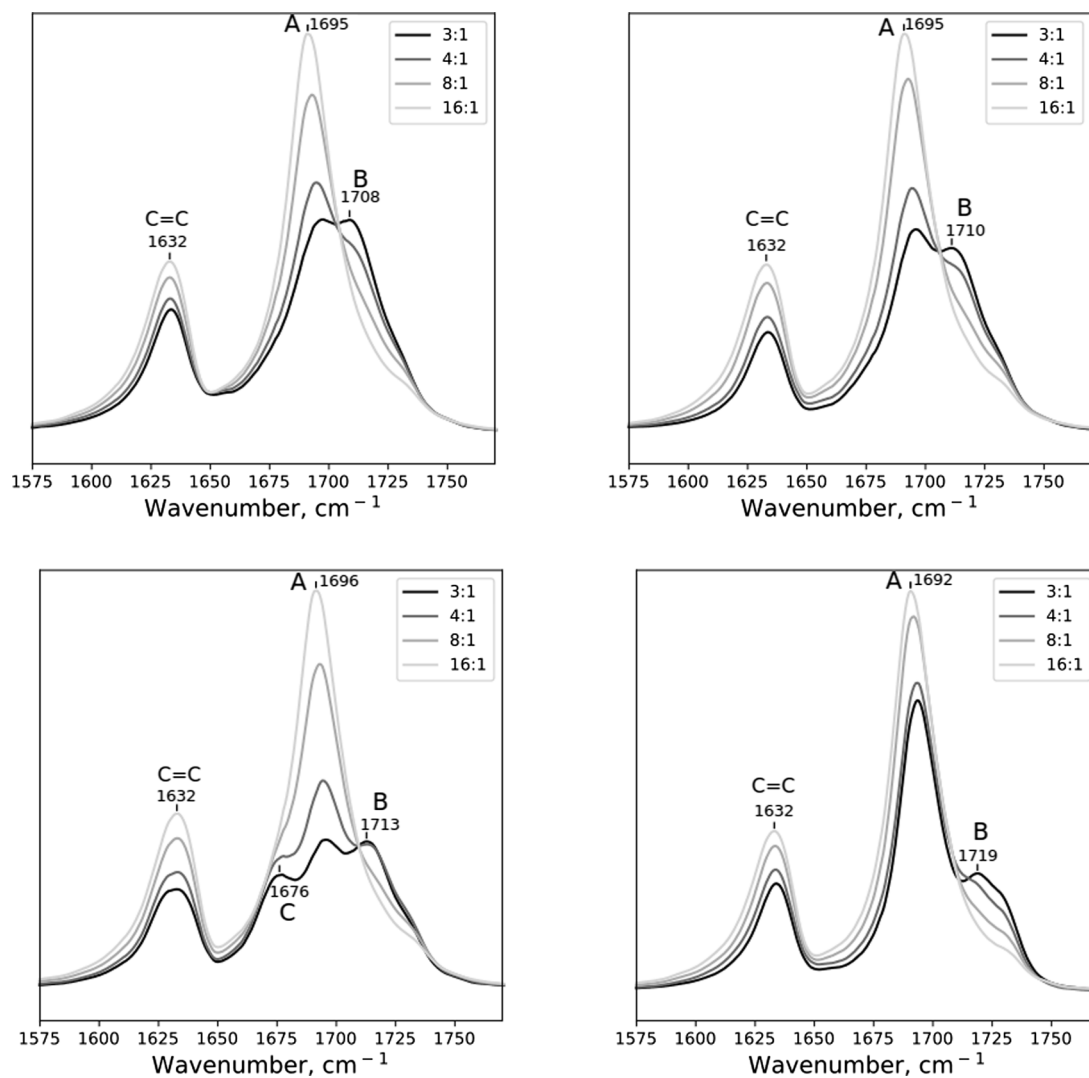
Fig. 3. Area-normalised ATR-IR absorption spectra in the range of 1570–1750 cm^{-1} for DEMs systems with different molar ratio of HBD:HBA: (a) TBAC, (b) TBANO, (c) TBAHS, (d) TBABF.
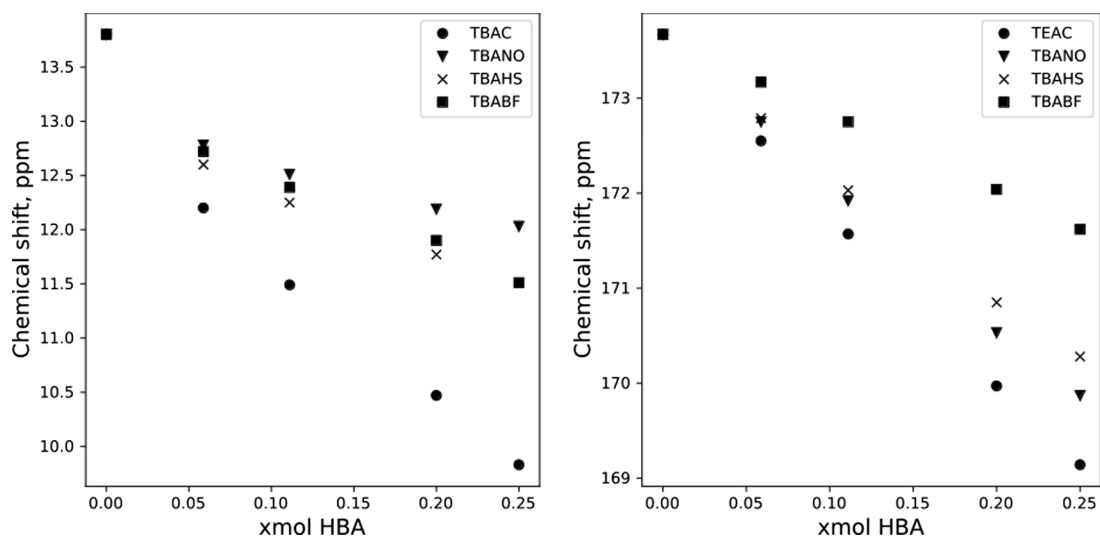

Fig. 4. Chemical shift of carboxylic MAA proton (a) and carboxylic carbon (b)in function of mole fraction of HBA.

complex [33].

Finally, as can be seen the Fig. 3 the band from stretching of double bond (1632 cm^{-1}) does not change position in DES systems in comparison to bulk MAA. No change in band position suggests that the formation of the MAA-DES complex has no impact on the vibrational energy of double bond.

3.3. ^1H and ^{13}C NMR

DEM mixtures were further analysed by NMR spectroscopy. This method is the most validate technique to study H-bond interactions due to the chemical shift of the carboxylic group is very sensitive to intermolecular interactions [34]. Measurements of neat samples were performed using a capillary containing D$_2$O as lock reference. The full spectra are shown in Supporting Information (Figs. S2 and S3).

Analysis of trends chemical shifts for different HBD:HBA molar ratios on NMR spectra could suggest the nature of molecular interactions in DES systems [35]. Chemical shifts of carboxylic proton and carboxylic carbon in the function of the molar fraction of HBA are presented in Fig. 4. A drift of the position of the chemical shift of the acidic MAA proton is a result of a change of concentration of cyclic dimers and complexed forms. The observed value of the shift is a weighted average between chemical shift proton in MAA dimer and in the DEM complex. Based on the direction of carboxylic proton chemical shift the H-bond strength between the carboxylic group and anions in tetrabutylammonium salts can be compared. As can be seen on Fig. 4a changes of the chemical shift of acidic proton are arranged linearly with the reverse slope with the increase of the molar ratio of HBA. The upfield shift of exchangeable proton signal indicates an increase in the shielding of acidic proton [36]. Drift of the carboxylic proton signal toward lower frequency in MAA-QX complex indicates lower H-bond energy compared to dimers. By anion type, the magnitude of the change is arranged as follows $Cl^- > HSO_4^- > BF_4^- > NO_3^-$, however, the effect caused by chloride anions diverges significantly from the others which is in line with relative high H-bonded acceptor properties for the anion [26].

It should be mentioned that the strength of H-bonds between MAA and QX estimated based on NMR measurements do not fully correlate with FTIR results. Both techniques indicate that hydrogen bonds with the highest strength are formed with chloride anion, but do not correlate with respect to the rest of the anions studied. A possible explanation of this observation may be the fact that chemical shift does not solely depend on H-bond acceptance properties of HBA but also on shielding properties of anion which affect changes in chemical shift of acidic proton [37].

To further analyse H-bond strength we have also employed ^{13}C NMR spectroscopy experiment. The signal from the carboxylic carbon is sensitive to H-bond interactions, and its chemical shift of the carboxylic carbon in the HBD correlates with the strength of the chemical bond [38,39]. It should also be pointed out that changes on the carbon spectrum are less responsive to shielding by unpaired electrons on anions in ammonium salts than carboxylic proton during ^1H NMR experiment. Chemical shifts of the signal corresponding to carboxyl carbon in MAA in the function of the molar fraction of the HBA are presented in Fig. 4b. As can be seen for all systems the upfield shift of the signal for carboxyl carbon correlates with the increasing concentration of HBA. In addition, the effect of anion type on the chemical shift of carboxyl carbon fully correlates with changes of the wavenumber of carbonyl band in the MAA-DES complex obtained by FTIR. Assuming that the determination of H-bond strength by FTIR and ^{13}C NMR experiments are more precise than ^1H NMR it should be stated that H-bonded acceptors properties for tetrabutylammonium salts anions are arranged in order $Cl^- > NO_3^- > SO_4H^- \gg BF_4^-$.

Interesting inferences can be drawn from the chemical shifts of vinyl atoms. Several examples can be found in the literature showing a correlation between the reactivity of unsaturated monomers and chemical
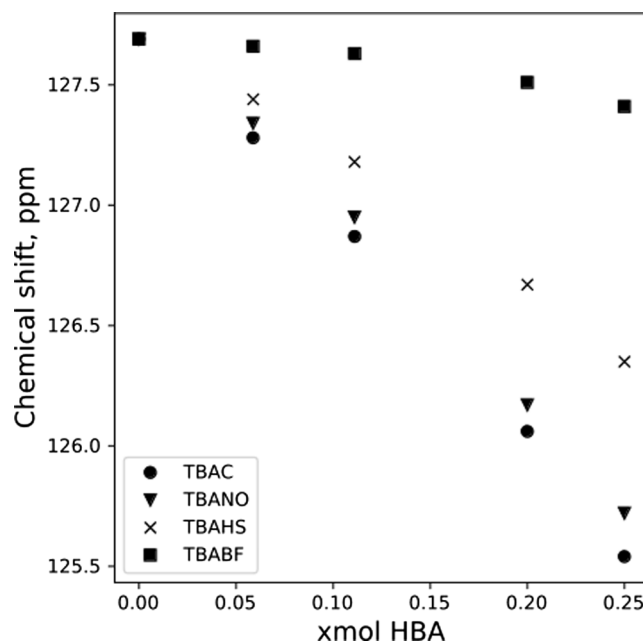

Fig 5. Chemical shift of unsaturated β-carbon of MAA in function of molar ratio of HBA.

shifts on ^1H and ^{13}C NMR spectra of vinyl atoms [40,41]. Typically, the reactivity of a monomer is determined by π-electron density on double bonds which strictly correlate with the chemical shift of vinyl protons and β-carbon [42]. Fig. 5 presents chemical shifts of β-carbon in the function of the molar ratio of HBA. As evident, the shift toward a higher field corresponds with an increase in the concentration of ammonium salts for all cases, which indicates an increase in π-electron density on β-carbon. Increasing electron density on double bond might indicate an increased reactivity in radical reaction of MAA-QX complex compared to bulk MAA. It should be emphasized that based on ^{13}C NMR experiments reactivity of DEMs can be arranged in order $Cl^- > NO_3^- > HSO_4^- \gg BF_4^-$, which strictly correlate with the strength of the H-bond. Moreover, the chemical shift of vinyl protons increases linearly with chemical shift of β-carbon (see Supplementary materials Fig. S4), which suggest that increase in π-electron density on β-carbon lead to a decrease in chemical shifts of vinyl protons [41]. The same conclusion can be made by analysing trends in chemical shifts of vinyl protons (Fig. S5).

3.4. Density

The literature provides examples of both contraction and expansion of density with increasing molar ratio of HBA to HBD. The most important factor affecting the density of DES are intermolecular interactions. An interesting example is glycerol-choline chloride systems. The presence of choline chloride disrupts to some extent the hydrogen bond network in pure glycerol resulting in an increase in molecular mobility and better molecule packing which lead to strong contraction with an increase of the molar ratio of choline chloride (HBA) [43]. The opposite effect can be observed in aurea-ZnCl$_2$ mixture when salt addition to pure urea lead to enhancements of vacancies concentration and thus expansion of density [44]. Density measurements of DEMs were conducted at 25 °C. The relationship between density and molar ratios of HBA is presented in Fig. 6 and summarized in Supplementary Materials Table S1. As can be seen density increases for mixtures composed of MAA-TBAHS and MAA-TBABF, while decreases for MAA-TBAC and MAA-TBANO systems. The differences in changes of density might be attributed to a different molecular organization or packing of the DEM components. The density reduction observed for MAA-TBAC and MAA-TBANO systems can be explained using free volume theory
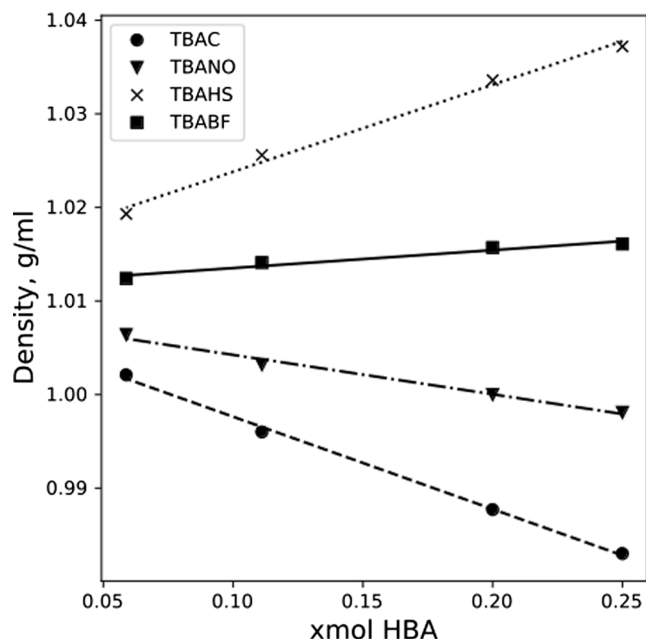
Fig. 6. Density of the MAA-DES systems in function of molar ratio of HBA. Lines are only for guide eyes. Lines are only for guide eyes.

Fig. 7. Viscosity of the MAA-DES systems in function of molar ratio of HBA. Lines are only for guide eyes.

[43]. As we mentioned above, Cl^- and NO_3^- anions form the most stable hydrogen-bonded MAA-QX. The complexes have increased mobility and better molecule packing compared to acidic cyclic dimers (and higher-order agglomerates of MAA) which lead to a decrease in density. This effect is caused by a similar phenomenon as in the glycerol–choline chloride system. In addition, it should be pointed out that the contraction effect caused by Cl^- is greater than NO_3^- and densities for the highest HBD:HBA (3:1) ratios are respectively 0.9830 g/ml for TBAC and 0.9981 g/ml for TBANO. It should be also said that these anions differ in thermochemical radii. The estimated thermochemical radii of Cl^- is 181 Å and the NO_3^- is 202 Å [45]. The difference in thermochemical radii of anions can also influence the degree of contraction. Densities of the systems including BF_4^- and HSO_4^- anions increase with an increase of the molar ratio of HBA. This phenomenon can be explained by the hole theory of DES [44]. Average hole radius decrease in MAA-QX complex which lead to an increase of the DES density. Furthermore, density expansion is much greater for HSO_4^- than BF_4^-, which for HBD:HBA (3:1) is 1.0372 g/ml for TBAHS and 1.0161 g/ml for TBABF. A potential explanation for observed variations might be the formation of complexes due to extra H-bond between $SO—H \cdots O=C$. Additional H-bond lead to better packing of molecules. In addition, HSO_4^- (223 Å) has slightly greater thermochemical radii than BF_4^- (211 Å), which may determine the expansion of density [45].

3.5. Viscosity

Viscosity is one of the key characteristics of the polymerizable system, due to the fact that it affects the termination and propagation rate. DES viscosity can be explained on the basis of intermolecular interactions and hole theory. In analogy to classic fluids viscosity of DES is related to free volume and the probability of movements of molecules to the free volume [46]. Viscosities of DEM mixtures were measured as a function of the molar ratio of HBA:HBD at 25 °C. The obtained results are presented in Fig. 7 and summarized in Table S2. As can be seen, viscosity increases with an increase in the molar ratio of HBA for all investigated systems. An increase in viscosity of DES is attributed to the formation of hydrogen bond network (MAA-QX complexes), which lead to a decrease in mobility of the species. For the highest analysed molar ratio HBD:HBA 3:1 viscosity shall be arranged in order: HSO_4^- (184 cP)

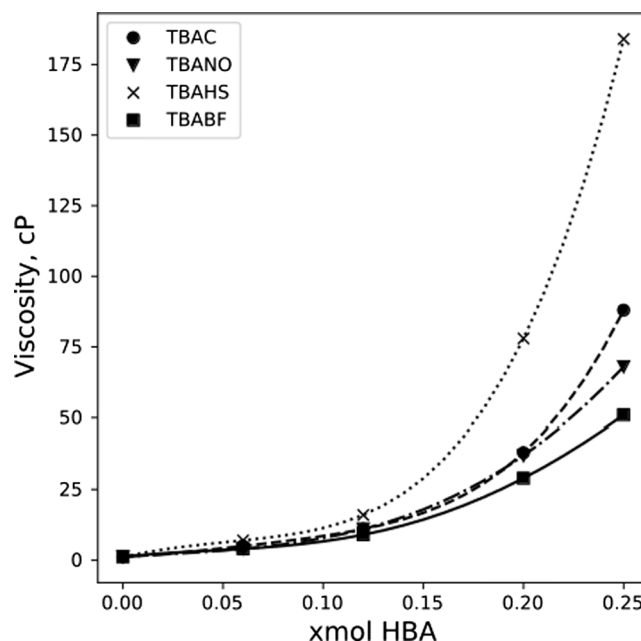$\gg Cl^-$ (88 cP) $> NO_3^-$ (68 cP) $> BF_4^-$ (51 cP). As evident, hydrogensulfate anion stands out significantly from the rest of anions studied. A possible explanation could be the ability of hydrogen sulphate anion to share of its acidic hydrogen and to form an extra hydrogen bond with a carboxylic group of MAA (or another HSO_4^- molecule). This leads to an increase in the attractive forces between molecules and thus making the liquid more viscous [47]. It is worth noting that higher viscosity values correlate with H-bond accepting properties of anions. Summarizing these studies, it can be stated that the viscosity in MAA – tetrabutylammonium salts mixtures depends on the number of hydrogen bond sites on the anion and HBA strength.

3.6. Photopolymerization by real time FTIR

RT-FTIR is a widely used technique for monitoring the light-initiated processes [19]. This method was used to follow the conversion of vinyl bonds in order to determine the effect of anion structure in HBA on the polymerization process. The obtained conversion curves have typical for auto accelerated processes sigmoidal shapes. At the beginning, a short induction period is observed due to the inhibition effect by MEHQ and traces of O_2 dissolved in MAA. At the end, the process is slowing down at a certain reaction time because of the glass effect, which leads to reduced macroradical mobility at high monomer conversion [48,49].

It is known that photopolymerization rate and induction period depend on light intensity and photoinitiator concentration. For our analyses, we used TPO as a photoinitiator with a concentration of 2 mg/ml, as its absorption spectrum is well separated from the monomer absorption spectrum. A low concentration of TPO was chosen to keep the optical absorbance at a low level and homogeneous optical properties. It should be noted that the polymerization of MAA-based DES is an exothermic process and proceeds rapidly, which lead to an increase in system temperature. The temperature rise promotes the segmental mobility of polymer chains and enhances the reactivity of radicals. One way to achieve isothermal conditions during the polymerization process is to minimize the light intensity, but this leads to a slower reaction and formation of polymers fractions with higher molecular weights that precipitate out during the initial phase of the reaction. In the initial studies, we observed that a significant temperature increase occurs even at low light intensities of the LED, so we conducted the experiment with
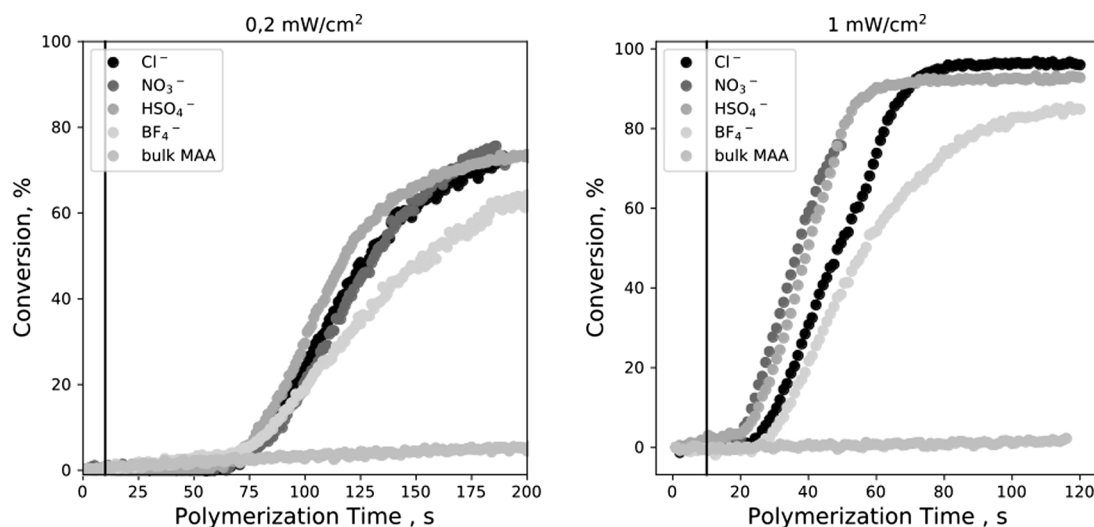
Fig. 8. Conversion curves vs irradiation time for HBD:HBA = 3:1 systems as well as MAA. (a) 0.2 mW/cm^2, (b) 1 mW/cm2. A vertical line marks the switching ON of the light time.

Table 1
Initial rate of photopolymerization reaction for HBD:HBA 3:1 as well as MAA determined on the basis of initial slopes of conversion curves.

Light intensity [mW/cm^2]	Anion type	Initial photopolymerization rate, s^{-1}
0.2	bulk MAA	no polymerization during 200 s of light irradiation
	Cl$^-$	0.92
	NO$_3^-$	0.96
	HSO$_4^-$	1.04
	BF$_4^-$	0.57
1	bulk MAA	no polymerization during 120 s of light irradiation
	Cl$^-$	2.13
	NO$_3^-$	2.87
	HSO$_4^-$	2.66
	BF$_4^-$	1.77

the following conditions: 0.2 mW/cm^2,1 mW/cm^2 and 19.8 mW/cm^2. The conversion versus irradiation time plots of the DEMs(HBD:HBA 3:1) are presented in Fig. 8 (other molar ratios in Supplementary Materials Fig. S6). Calculated rates taken from initial slopes are presented in Table 1 (and Supplementary Materials TableS3).

Due to the fact that the poly(methacrylic acid) precipitates from the monomer, it is difficult to achieve high conversion in bulk MAA. Zhou et al. reported that maximum conversion for bulk MAA can reach up to 60% [50]. As can be seen in conversion plots, polymerization of MAA as DEM leads to increased conversion up to 70–90%. A possible explanation for this phenomenon is the solvation of poly(MAA) by the quaternary ammonium salt, which inhibits the precipitation of the polymer to some extent and limits the trapping of active radicals in a separated solid phase. As shown in Table 1initial polymerization rates for DEM with different type of anion are arranged in order HSO$_4^-$ > NO$_3^-$ > Cl$^-$ > BF$_4^-$ for 0.2 mW/cm^2. and NO$_3^-$ > HSO$_4^-$ > Cl$^-$ ≫ BF$_4^-$for 1 mW/cm^2.

It has been known that higher viscosity leads to an increase in the polymerization rate [51]. However, despite the significantly higher viscosity of MAA-TBAHS than other investigated DEMs, no significant increase in initial polymerization rate is observed, which lead to the conclusion that the viscosity is not crucial in the analysed cases. The second factor determining the rate of polymerization in DES is a molecular organization of the monomer e.g. degree of dimerization. Topchiev et al. showed that MAA polymerizes faster in monomeric form than as hydrogen-bonded cyclic dimer [52]. Based on this, we postulate

that the key factor influencing polymerization rate is the efficiency of the formation of a monomeric complex between MAA and QX. The formation of monomeric complexes might reduce repulsive interactions between monomers, leading to increased reactivity. Systems containing TBAHS, TBAC and TBANO show similar initial polymerization rates, in contrast to TBABF, where a significant lower polymerization rate is observed. As we mentioned earlier BF$_4^-$ anion is the weaker HBA studied and concentration of the uncompleted form of MAA, i.e. dimers in MAA-TBABF systems is the highest among all salts investigated.

For a more complete analysis of the photopolymerizationof DEMs systems, we calculated the reaction rate as a function of reaction time. The rate was calculated by differentiating the sigmoidal function fitted to the monomer conversion. In addition, in order to determine the effect of temperature increase on reaction rate we completed our experiments by measuring the temperature profile during irradiation time. Fitted models are presented in Supplementary Materials in Fig. S7. Fig. 9 presents the obtained results and temperature profile for 0.2 mW/cm^2 and 1 mW/cm^2 light intensity (Fig. S8 for 19.8 mW/cm^2). As can be seen, a significant decrease of R$_p^{max}$ is observed for the system containing BF$_4^-$ salt. The R$_p^{max}$ for DEM based on NO$_3^-$ salt is more than twice than BF$_4^-$ -based DEM for both 0.2 mW/cm^2 and 1 mW/cm^2. In addition, it should be noted that the course of change of the reaction rate for tetrafluoroborate anion is considerably milder which is determined by the slow temperature rise and the significantly lower T$_{max}$ (53 °C – 0.2 mW/cm^2 and 78 °C – 1 mW/cm) reached during the photopolymerization. For lower light intensity (0.2 mW/cm^2) there is no significant difference for systems containing NO$_3^-$, HSO$_4^-$ and Cl$^-$ anions both in R$_p^{max}$ and T$_{max}$. For 1 mW/cm^2 we can note significant changes in comparison to 0.2 mW/cm^2.R$_p^{max}$ for NO$_3^-$ and HSO$_4^-$ are very similar while the maximum rate for Cl$^-$ is much lower. Additionally, it should be noted that MAA-TBAC achieves higher T$_{max}$ (97 °C) than MAA-TBAHS (94 °C) and MAA-TBANO (86 °C). R$_p^{max}$ correlates with initial rates designated on the base of the initial slope of the conversion curve. On this basis, it can be concluded that tetrabutylammonium salts containing NO$_3^-$ and HSO$_4^-$ anions form complexes with MAA polymerizing at similar rates, a slightly lower photopolymerization rate is observed for the system with Cl$^-$, while the MAA-QX complex with BF$_4^-$ anion polymerizes the slowest.

Polymerization of monomer-based DES results in the formation of solid materials (PDEM) containing polymer, unreacted monomer and ammonium salt. The PDEMs obtained by photopolymerization of mixtures of MAA with the ammonium salts show a different appearance (Figs. 10 and S9). Depending on the composition of DEM and the light
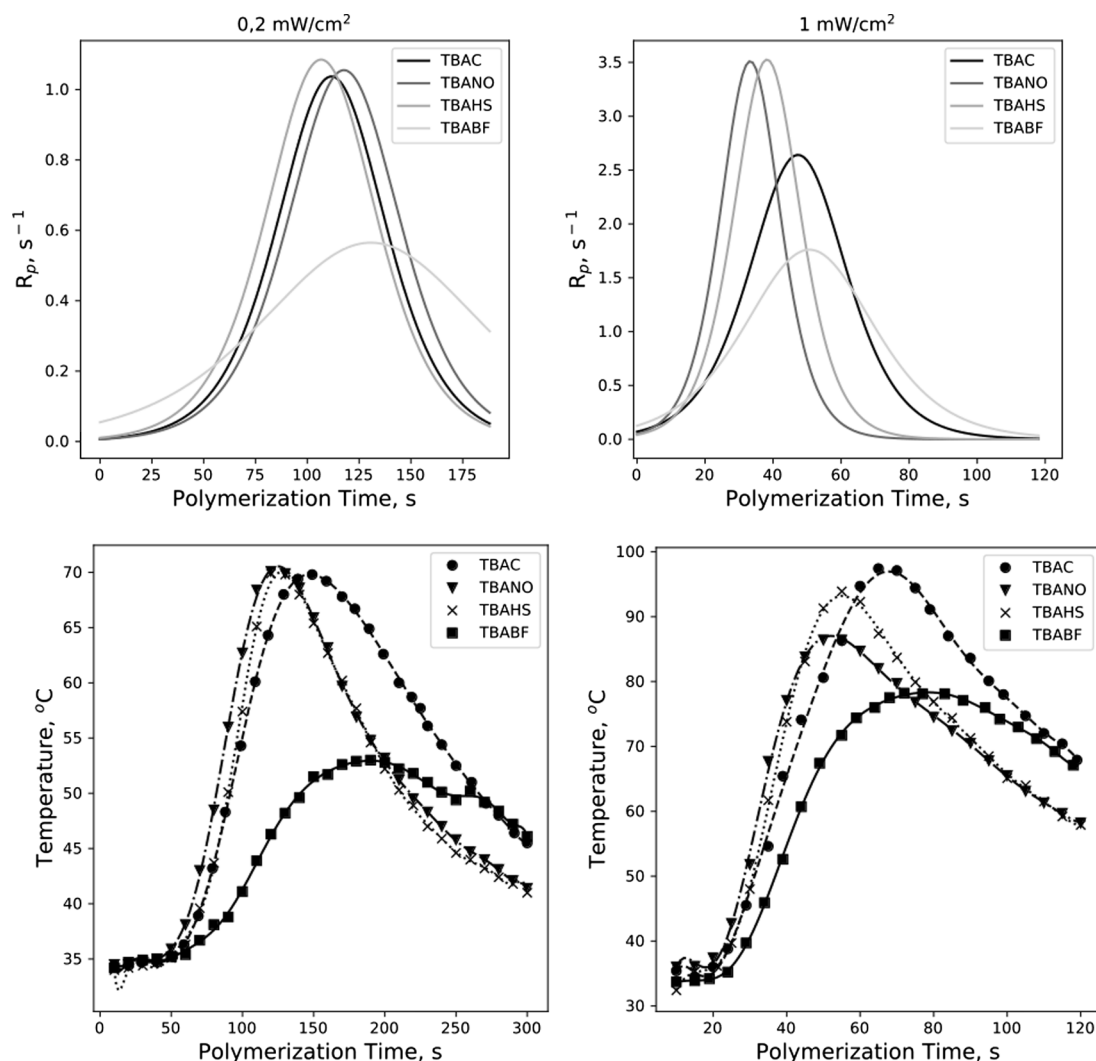
Fig. 9. (a) Rate of polymerization vs irradiation time for light intensity 0.2 mW/cm^2 (b) Rate of polymerization vs irradiation time for light intensity 1 mW/cm^2, (c) temperature profile vs irradiation time for light intensity 0.2 mW/cm^2, (d) temperature profile vs irradiation time for light intensity 1 mW/cm^2. For HBD:HBA – 3:1 systems. Lines are only for guide the eyes.
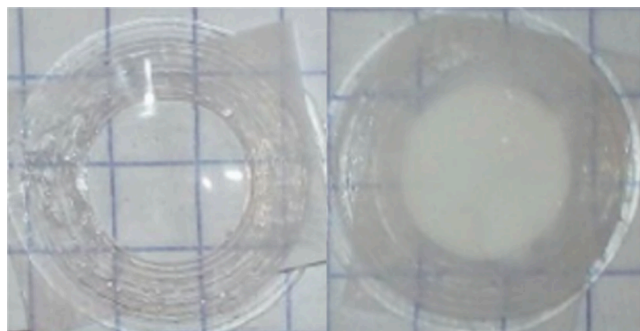
Fig. 10. Appearance of PDES: (a) transparent (PDES MAA:TBAHS 3:1, 19.8 mW/cm^2) and (b) cloudy (PDES MAA:TBABF 3:1, 19.8 mW/cm^2).

intensity used for initiation of photopolymerization, PDEMs are transparent and tough (glass-like) or cloudy and brittle (see Fig. 10). The obtained results indicate that higher content of ammonium salt in DEM (molar ratios 3:1 and 4:1) and higher light intensity during photopolymerization (19.8 mW/cm^2) promote the formation of glass-like PDEM. An exception is the MAA:TBABF system which acquires the cloudy state regardless of the initial composition of DEM MAA:TBABF

and the light intensity used for photopolymerization. As shown by FTIR analysis, the H-bond between MAA and TBABF are the weakest among the quaternary ammonium salts tested, so it is likely that these interactions are insufficient to solubilize poly(MAA) formed, which might be a reason of phase separation. PDEM with low ammonium salt content (molar ratios of 8:1 and 16:1) generally have a cloudy appearance. These systems behave like bulk MAA, probably because of too small amount of the salt, which results in the precipitation of poly(MAA) in the system, as it occurs in bulk MAA [53–55]. However, when MAA is polymerized in DEM with high ammonium salt content, e.g. MAA:choline chloride (1.6:1 and 2:1) and MAA:lidocaine (3:1) molar ratio, a transparent polymeric material are obtained [17,30].

Compared to other DEMs, MAA:TBAHS stands out in terms of obtaining transparent PDEM, which retains glass-like properties after polymerization in the widest range of concentrations and photopolymerization light intensity used. MAA:TBAHS DEM (molar ratios of 3:1 and 4:1) is the only one to form transparent PDEM when using a light intensity of 1 mW/cm^2 for photopolymerization. It is possible that the higher solubilisation of poly(MAA) by TBAHS is due to extra hydrogen bonds between the carboxylic groups of the polymer and hydrogen sulfate anion presented in the mixture. At present, it is not clear why the higher light intensity during photopolymerization, and therefore the faster polymerization process and the higher maximal temperature that

the sample achieves, promote the preparation of glass-like PDEM.

3.7. SEC analysis

To determine the effect of the anion structure in HBA on the molecular weight of poly(MAA) formed in photopolymerization reactions we performed SEC analysis. The results i.e. number and weight average molecular weight, polydispersity index values and molecular weights distributions are collected in supplementary materials (Table S4, Figs. S14–S15).

Fig. 11a shows weight average molecular weight as the function of molar ratio of HBA for polymers synthesized under 1 mW/cm2 light intensity. The molecular weights of formed polymers increase with increasing HBA concentration. The greatest effect of the increase is observed for HSO_4^-, whereas BF_4^- has the weakest influence. Since molecular weights of polymers formed by radical polymerization depend on many factors it is not easy to find out the clear effect of anion structure in HBA on molecular weight of polymer produced. However, it should be noted that the increase in molecular weights correlates with hydrogen bond acceptor properties of the analysed anions reported in previous sections by FTIR and NMR experiments.

It can be seen that for most of the analysed systems, polymers formed in the presence of BF_4^- anion featuring the lowest polydispersity and molecular weight (Fig. 11b). A possible explanation for this phenomenon is the weakest coordination level of MAA by BF_4^- anion, which lead to relative fast precipitation of poly(MAA) from monomer and trapping the propagating macroradicals in a separated solid phase. The opposite effect can be observed for HSO_4^-, which is the anion with the best coordinating properties of the MAA and the polymerization reaction takes the longest time in the liquid phase.

3.8. Time-resolved EPR

In the present study, the Time-Resolved EPR method was applied to investigate the influence of the type of tetrabutylammonium salt anion on the relative termination rate of photopolymerization of DEM. The EPR experiments were conducted in bulk systems and without the addition of spin traps. Fig. 12 shows an example of full EPR spectra presenting the propagating poly(methacrylic acid) macroradical. The structure of the spectra agrees with published measurements [56].

The aim of the measurements was to determine qualitatively relative rates of the termination of polymerization for the investigated DEM systems. Since the intensity of the EPR signal is proportional to the
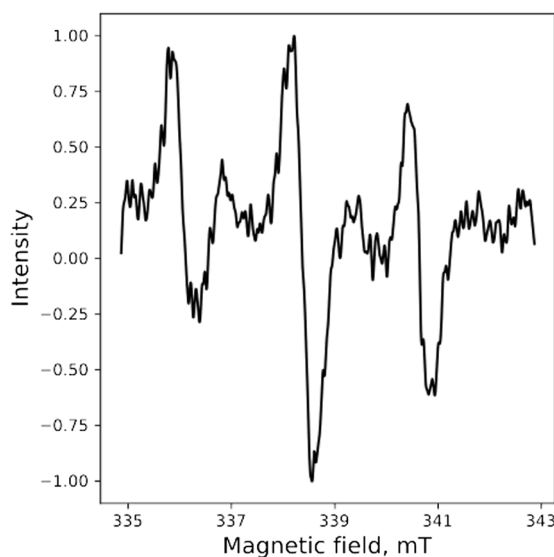

Fig. 12. EPR spectra of the propagating poly(methacrylic acid) macroradical generated in MAA-TBAC system.

concentration of radicals, the radicals generation/consumption rate can be determined from the intensity of the EPR signal. The relative termination rates where estimated on the basis of the decay on the central line of EPR spectra after a short flash of light. For bulk systems, in which the polymer is not soluble in its monomer and precipitates, radicals are going to be trapped in a separated phase, which strongly reduces the possibility of termination and keeps the EPR signal at a constant level for a long time [57]. Phase separation makes also the overall system more complex and the EPR measurements more difficult to quantitative interpretation.

In order to make the results independent on the initial radical concentration, the amplitude values at each time were divided by the maximum amplitude recorded for each system. The linear range of decreasing amplitude vs time is shown in Fig. 13, whereas raw EPR data are presented in Fig. S10. The relative rate of termination was determined from reverse the slope of the amplitude decays and the results are listed in Table 2. As can be seen, the structure of the salt anion affects the relative rate of termination, which follows the order: HSO_4^- >NO_3^- >Cl^- >BF_4^-. It is not clear what contributes to the different relative
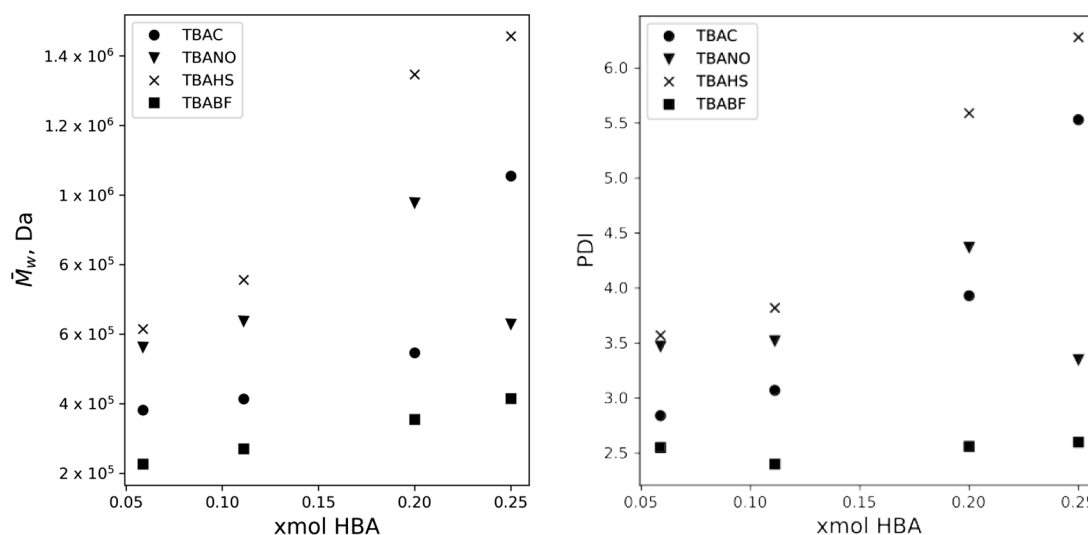

Fig. 11. (a) Weight average molecular weight of poly(MAA) synthesized under 1 mW/cm^2 light intensity in function of molar ratio of HBA, (b) Polydispersity index of poly(MAA) synthesized under 1 mW/cm2 light intensity in function of molar ratio of HBA.
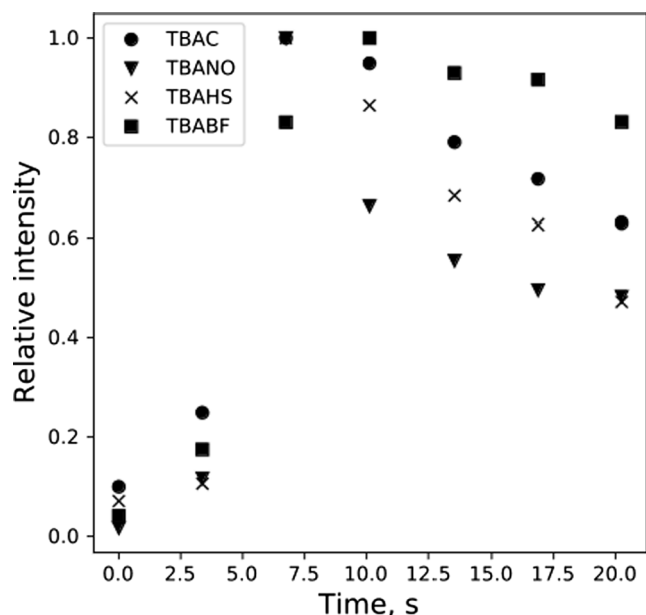
Fig. 13. Linear range of relative intensity decay of EPR spectra vs time.

Table 2
Slopes of of decreasing EPR signal amplitude in linear range for HBD:HBA 3:1.

Anion type	Slope of decreasing EPR signal amplitude
Cl^-	−0.029
NO_3^-	−0.036
HSO_4^-	−0.038
BF_4^-	−0.015

termination rates, but one reason for the reduced chain growth termination is the reduced mobility of precipitated macroradicals. As mentioned above, the solubility of the polymer in MAA-DES depends on the type of ammonium salt anion. Extra H-bonding site provided by the HSO_4^- anion increase the solubility of poly(methacrylic acid), which enhances the mobility of macroradicals and keeps the higher probability of termination. The opposite effect is evident in systems with BF_4^- anion. Weak interactions through H-bond with poly(MAA) reduces the solubility of the macromolecules in DEM and leads probably to early precipitation of macroradicals, that are trapped by phase separation, which significantly reduces the probability of termination.

4. Conclusions

A range of Deep Eutectic Monomers based on methacrylic acid and tetrabutylammonium salts with different anions (Cl^-, NO_3^-, HSO_4^- and BF_4^-) have been prepared and investigated using spectroscopic methods. Dissociation of MAA dimers and formation of HBD-HBA molecular complexes between MAA and the anions were proven. Based on FTIR spectroscopy it could be concluded that Cl^-, NO_3^- and HSO_4^- coordinate MAA at a similar level, whereas BF_4^- presents much lower hydrogen-bond acceptor strength. However, both FTIR and NMR data indicate that H-bonds formed between MAA and tetrabutylammonium salts are weaker than in H-bonds in MAA cyclic dimers. Interestingly, HSO_4^- anion demonstrates the ability to acts both as HBD (sharing its acidic proton) and HBA, which results in the formation of cyclic and higher order, resonance-stabilized complexes with MAA, demonstrating higher hydrogen-bond strength than in the dimeric state. This effect is presumably an explanation of the much higher viscosity of MAA-TBAHS mixtures compared with the other systems studied.

The photopolymerization results presented here suggest that the main factor influencing the radical polymerization of DEMs is the hydrogen-bond accepting strength of the anion. Systems containing weekly coordinating BF_4^- anions show the lowest both initial photopolymerization rate and maximum rate. In contrast to NMR findings, showing an increase in electron density on the vinyl group of MAA in DEMs what should lead to enhanced reactivity of MAA, the other anions have a little bit ambiguous but rather a similar effect on the photopolymerization rate. Contrary to expectations, also the significantly higher viscosity of MAA-TBAHS mixtures seems to be a negligible factor, not affecting the process rate. EPR studies proved the presence of long-living radicals trapped in polymerization products. However, the results are qualitative and it is difficult to conclude what is the effect of anion structure on termination rate, and thus radicals lifetime.

In conclusion, we demonstrated that the chemical structure of hydrogen-bond acceptor anion determines intermolecular interactions with acidic monomer in DEMs, and thus impacts course of radical polymerization. It seems that the effect of cation type could be less pronounced, but this hypothesis will be examined in our future work.

Data availability

The raw/processed data required to reproduce these findings cannot be shared at this time due to technical or time limitations.

CRediT authorship contribution statement

Samuel Wierzbicki: Conceptualization, Validation, Formal analysis, Investigation, Data curation, Writing – original draft, Writing – review & editing, Visualization. **Kacper Mielczarek:** Formal analysis, Investigation. **Monika Topa-Skwarczyńska:** Methodology, Investigation. **Krystian Mokrzyński:** Methodology, Investigation. **Joanna Ortyl:** Conceptualization, Methodology, Investigation. **Szczepan Bednarz:** Conceptualization, Validation, Formal analysis, Investigation, Data curation, Writing – original draft, Writing – review & editing.

Declaration of Competing Interest

The authors declare that they have no known competing financial interests or personal relationships that could have appeared to influence the work reported in this paper.

Appendix A. Supplementary material

Supplementary data to this article can be found online at https://doi.org/10.1016/j.eurpolymj.2021.110836.

References

[1] E.L. Smith, A.P. Abbott, K.S. Ryder, Deep eutectic solvents (DESs) and their applications, Chem. Rev. 114 (21) (2014) 11060–11082, https://doi.org/10.1021/cr300162p.

[2] Q. Zhang, K. De Oliveira Vigier, S. Royer, F. Jérôme, Deep eutectic solvents: syntheses, properties and applications, Chem. Soc. Rev. 41 (2012) 7108–7146, https://doi.org/10.1039/c2cs35178a.

[3] A. Paiva, R. Craveiro, I. Aroso, M. Martins, R.L. Reis, A.R.C. Duarte, Natural deep eutectic solvents – solvents for the 21st century, ACS Sustain. Chem. Eng. 2 (5) (2014) 1063–1071, https://doi.org/10.1021/sc500096j.

[4] D.J.G.P. Van Osch, C.H.J.T. Dietz, S.E.E. Warrag, M.C. Kroon, The curious case of hydrophobic deep eutectic solvents: a story on the discovery, design, and applications, ACS Sustain. Chem. Eng. 8 (2020) 10591–10612, https://doi.org/10.1021/acssuschemeng.0c00559.

[5] B.D. Ribeiro, C. Florindo, L.C. Iff, M.A.Z. Coelho, I.M. Marrucho, Menthol-based eutectic mixtures: hydrophobic low viscosity solvents, ACS Sustain. Chem. Eng. 3 (10) (2015) 2469–2477, https://doi.org/10.1021/acssuschemeng.5b00532.

[6] C.H.J.T. Dietz, M.C. Kroon, M. Di Stefano, M. van Sint Annaland, F. Gallucci, Selective separation of furfural and hydroxymethylfurfural from an aqueous solution using a supported hydrophobic deep eutectic solvent liquid membrane, Faraday Discuss. 206 (2018) 77–92, https://doi.org/10.1039/C7FD00152E.

[7] D.J.G.P. van Osch, D. Parmentier, C.H.J.T. Dietz, A. van den Bruinhorst, R. Tuinier, M.C. Kroon, Removal of alkali and transition metal ions from water with hydrophobic deep eutectic solvents, Chem. Commun. 52 (80) (2016) 11987–11990, https://doi.org/10.1039/C6CC06105B.

[8] J.D. Mota-Morales, R.J. Sánchez-Leija, A. Carranza, J.A. Pojman, F. del Monte, G. Luna-Bárcenas, Free-radical polymerizations of and in deep eutectic solvents: green synthesis of functional materials, Prog. Polym. Sci. 78 (2018) 139–153, https://doi.org/10.1016/j.progpolymsci.2017.09.005.

[9] M. Isik, F. Ruiperez, H. Sardon, A. Gonzalez, S. Zulfiqar, D. Mecerreyes, Innovative poly(Ionic liquid)s by the polymerization of deep eutectic monomers, Macromol. Rapid Commun. 37 (2016) 1135–1142, https://doi.org/10.1002/marc.201600026.

[10] M. Isik, S. Zulfiqar, F. Edhaim, F. Ruiperez, A. Rothenberger, D. Mecerreyes, Sustainable poly(Ionic Liquids) for CO2 capture based on deep eutectic monomers, ACS Sustain. Chem. Eng. 4 (12) (2016) 7200–7208, https://doi.org/10.1021/acssuschemeng.6b0213710.1021/acssuschemeng.6b02137.s001.

[11] D. Carriazo, M.C. Serrano, M.C. Gutiérrez, M.L. Ferrer, F. del Monte, Deep eutectic solvents in polymerizations: a greener alternative to conventional syntheses, Chem. Soc. Rev. 41 (2012) 4996–5014, https://doi.org/10.1039/c2cs15353j.

[12] M. Jablonský, A. Škulcová, J. Šima, Use of deep eutectic solvents in polymer chemistry–a review, Molecules 24 (2019) 1–33, https://doi.org/10.3390/molecules24213978.

[13] Y. Nahar, S.C. Thickett, Greener, faster, stronger: the benefits of deep eutectic solvents in polymer and materials science, Polymers (Basel) 13 (2021) 1–24, https://doi.org/10.3390/polym13030447.

[14] L.C. Tomé, D. Mecerreyes, Emerging ionic soft materials based on deep eutectic solvents, J. Phys. Chem. B 124 (39) (2020) 8465–8478, https://doi.org/10.1021/acs.jpcb.0c04769.

[15] J.D. Mota-Morales, E. Morales-Narváez, Transforming nature into the next generation of bio-based flexible devices: new avenues using deep eutectic systems, Matter. 4 (7) (2021) 2141–2162, https://doi.org/10.1016/j.matt.2021.05.009.

[16] J. Wang, S. Zhang, Z. Ma, L. Yan, Deep eutectic solvents eutectogels: progress and challenges, Green Chem. Eng. (2021), https://doi.org/10.1016/j.gce.2021.06.001.

[17] J.D. Mota-Morales, M.C. Gutiérrez, I.C. Sanchez, G. Luna-Bárcenas, F. Del Monte, Frontal polymerizations carried out in deep-eutectic mixtures providing both the monomers and the polymerization medium, Chem. Commun. 47 (2011) 5328–5330, https://doi.org/10.1039/c1cc10391a.

[18] J. Wang, Z. Ma, Y. Wang, J. Shao, L. Yan, Ultra-stretchable, self-healing, conductive, and transparent PAA/DES ionic gel, Macromol. Rapid Commun. 42 (2) (2021) 2000445, https://doi.org/10.1002/marc.v42.210.1002/marc.202000445.

[19] E. Andrzejewska, Photoinitiated polymerization in ionic liquids and its application, Polym. Int. 66 (3) (2017) 366–381, https://doi.org/10.1002/pi.2017.66.issue-310.1002/pi.5255.

[20] R. Li, G. Chen, M. He, J. Tian, B. Su, Patternable transparent and conductive elastomers towards flexible tactile/strain sensors, J. Mater. Chem. C 5 (33) (2017) 8475–8481, https://doi.org/10.1039/C7TC02703F.

[21] R. Li, K. Zhang, G. Chen, B. Su, M. He, Stiff, self-healable, transparent polymers with synergetic hydrogen bonding interactions, Chem. Mater. 33 (13) (2021) 5189–5196, https://doi.org/10.1021/acs.chemmater.1c01242.

[22] H. Qin, M.J. Panzer, Chemically cross-linked poly(2-hydroxyethyl methacrylate)-supported deep eutectic solvent gel electrolytes for eco-friendly supercapacitors, ChemElectroChem. 4 (10) (2017) 2556–2562, https://doi.org/10.1002/celc.v4.1010.1002/celc.201700586.

[23] B. Joos, J. Volders, R.R. da Cruz, E. Baeten, M. Safari, M.K. Van Bael, A.T. Hardy, Polymeric backbone eutectogels as a new generation of hybrid solid-state electrolytes, Chem. Mater. 32 (9) (2020) 3783–3793, https://doi.org/10.1021/acs.chemmater.9b05090.

[24] M.W. Logan, S. Langevin, B. Tan, A.W. Freeman, C. Hoffman, D.B. Trigg, K. Gerasopoulos, UV-cured eutectic gel polymer electrolytes for safe and robust Li-ion batteries, J. Mater. Chem. A. 8 (17) (2020) 8485–8495, https://doi.org/10.1039/D0TA01901A.

[25] K.F. Fazende, D.P. Gary, J.D. Mota-Morales, J.A. Pojman, Kinetic Studies of photopolymerization of monomer-containing deep eutectic solvents, Macromol. Chem. Phys. 221 (6) (2020) 1900511, https://doi.org/10.1002/macp.v221.610.1002/macp.201900511.

[26] S.J. Pike, J.J. Hutchinson, C.A. Hunter, H-bond acceptor parameters for anions, J. Am. Chem. Soc. 139 (19) (2017) 6700–6706, https://doi.org/10.1021/jacs.7b0200810.1021/jacs.7b02008.s001.

[27] M. Lim, R.M. Hochstrasser, Unusual vibrational dynamics of the acetic acid dimer, J. Chem. Phys. 115 (16) (2001) 7629–7643, https://doi.org/10.1063/1.1404144.

[28] H. Susi, The strength of hydrogen bonding: infrared spectroscopy, Methods Enzymol. 26 (1972) 381–391, https://doi.org/10.1016/S0076-6879(72)26019-0.

[29] J.J. Max, C. Chapados, Infrared spectroscopy of aqueous carboxylic acids: comparison between different acids and their salts, J. Phys. Chem. A 108 (2004) 3324–3337, https://doi.org/10.1021/jp036401t.

[30] J.D. Mota-Morales, M.C. Gutiérrez, M.L. Ferrer, I.C. Sanchez, E.A. Elizalde-Peña, J. A. Pojman, F.D. Monte, G. Luna-Bárcenas, Deep eutectic solvents as both active fillers and monomers for frontal polymerization, J. Polym. Sci. Part A Polym. Chem. 51 (8) (2013) 1767–1773, https://doi.org/10.1002/pola.26555.

[31] J.D. Mota-Morales, M.C. Gutiérrez, M.L. Ferrer, R. Jiménez, P. Santiago, I. C. Sanchez, M. Terrones, F. Del Monte, G. Luna-Bárcenas, Synthesis of macroporous poly(acrylic acid)–carbon nanotube composites by frontal polymerization in deep-eutectic solvents, J. Mater. Chem. A. 1 (12) (2013) 3970, https://doi.org/10.1039/c3ta01020a.

[32] H. Zhao, Q. Zhang, L. Du, Hydrogen bonding in cyclic complexes of carboxylic acid-sulfuric acid and their atmospheric implications, RSC Adv. 6 (75) (2016) 71733–71743, https://doi.org/10.1039/C6RA16782A.

[33] M. Rozenberg, A. Loewenschuss, Y. Marcus, An empirical correlation between stretching vibration redshift and hydrogen bond length, Phys. Chem. Chem. Phys. 2 (2000) 2699–2702, https://doi.org/10.1039/b002216k.

[34] M.D. Joesten, Hydrogen bonding and proton transfer, J. Chem. Educ. 59 (1982) 362–366, https://doi.org/10.1021/ed059p362.

[35] H. Wang, S.P. Kelley, J.W. Brantley, G. Chatel, J. Shamshina, J.F.B. Pereira, V. Debbeti, A.S. Myerson, R.D. Rogers, Ionic fluids containing both strongly and weakly interacting ions of the same charge have unique ionic and chemical environments as a function of ion concentration, ChemPhysChem. 16 (5) (2015) 993–1002, https://doi.org/10.1002/cphc.v16.510.1002/cphc.201402894.

[36] S.K. Davidowski, F. Thompson, W. Huang, M. Hasani, S.A. Amin, C.A. Angell, J. L. Yarger, NMR characterization of ionicity and transport properties for a series of diethylmethylamine based protic ionic liquids, J. Phys. Chem. B. 120 (18) (2016) 4279–4285, https://doi.org/10.1021/acs.jpcb.6b0120310.1021/acs.jpcb.6b01203.s002.

[37] K. Fujimori, G.T. Trainor, M.J. Costigan, Complexation and rate of polymerization of acrylic and methacrylic acid in the presence of poly(4-vinylpyridine) in dilute methanol solution, J. Polym. Sci. Polym. Chem. Ed. 22 (1984) 2479–2487, https://doi.org/10.1002/pol.1984.170221016.

[38] M.-C. Moreau-Descoings, F. Guillaume-Vilport, J.-P. Seguin, R. Uzan, J.-P. Doucet, Relationship between OH stretching frequencies of phenol-π- OR n-bases complexes and the chemical shifts of phenolic carbons, J. Mol. Struct. 127 (3-4) (1985) 297–303, https://doi.org/10.1016/0022-2860(85)80012-0.

[39] M.C. Moreau Descoings, F. Halabi, G. Goethals, J.P. Seguin, J.P. Doucet, 13c nmr measurement of hydrogen bonding effects for benzylic alcohol-πor n base complexes: relationship between the oh stretching frequencies and the chemical shifts of proton donor groups, Spectrosc. Lett. 20 (1987) 351–363, https://doi.org/10.1080/00387018708081556.

[40] J.J. Herman, P. Teyssie, Determination of vinyl monomers reactivity by carbon-13 nuclear magnetic resonance spectroscopy, Macromolecules 11 (1978) 839–840.

[41] K. Hatada, T. Kitayama, T. Nishiura, W. Shibuya, Relation between the reactivities of vinyl monomers in ionic polymerizations and their 1H NMR spectra, J. Polym. Sci. Part A Polym. Chem. 40 (13) (2002) 2134–2147, https://doi.org/10.1002/(ISSN)1099-051810.1002/pola.v40:1310.1002/pola.10296.

[42] V.M. Sutyagin, V.P. Lopatinskii, V.D. Filimonov, Relation between chemical shift values in 1H and 13C NMR spectra of vinyl monomers and some parameters of their reactivity in radical polymerization and copolymerization, Polym. Sci. U.S.S. R. 24 (9) (1982) 2252–2258, https://doi.org/10.1016/0032-3950(82)90286-6.

[43] A.P. Abbott, R.C. Harris, K.S. Ryder, Application of hole theory to define ionic liquids by their transport properties, J. Phys. Chem. B. 111 (18) (2007) 4910–4913, https://doi.org/10.1021/jp0671998.

[44] A.P. Abbott, J.C. Barron, K.S. Ryder, D. Wilson, Eutectic-based ionic liquids with metal-containing anions and cations, Chem. - A Eur. J. 13 (22) (2007) 6495–6501, https://doi.org/10.1002/(ISSN)1521-376510.1002/chem.v13:2210.1002/chem.200601738.

[45] M.C. Simoes, K.J. Hughes, D.B. Ingham, L. Ma, M. Pourkashanian, Estimation of the thermochemical radii and ionic volumes of complex ions, Inorg. Chem. 56 (13) (2017) 7566–7573, https://doi.org/10.1021/acs.inorgchem.7b0120510.1021/acs.inorgchem.7b01205.s001.

[46] A.P. Abbott, Application of hole theory to the viscosity of ionic and molecular liquids, ChemPhysChem. 5 (8) (2004) 1242–1246, https://doi.org/10.1002/(ISSN)1439-764110.1002/cphc.v5:810.1002/cphc.200400190.

[47] B.-Y. Zhao, P. Xu, F.-X. Yang, H. Wu, M.-H. Zong, W.-Y. Lou, Biocompatible deep eutectic solvents based on choline chloride: characterization and application to the extraction of Rutin from Sophora japonica, ACS Sustain. Chem. Eng. 3 (11) (2015) 2746–2755, https://doi.org/10.1021/acssuschemeng.5b00619.

[48] C. Decker, K. Moussa, Real-time kinetic study of laser-induced polymerization, Macromolecules 4462 (1989) 4455–4462.

[49] D.S. Achilias, A review of modeling of diffusion controlled polymerization reactions, Macromol. Theory Simulat. 16 (4) (2007) 319–347, https://doi.org/10.1002/(ISSN)1521-391910.1002/mats.v16:410.1002/mats.200700003.

[50] H. Zhou, Q. Li, T.Y. Lee, C.A. Guymon, E.S. Jönsson, C.E. Hoyle, Photopolymerization of acid containing monomers: real-time monitoring of polymerization rates, Macromolecules 39 (2006) 8269–8273, https://doi.org/10.1021/ma061332c.

[51] B.W. Brooks, Viscosity effects in free-radical polymerization of methyl methacrylate, Proc. R Soc. Lond. Ser. A. 357 (1977) 183–192, https://doi.org/10.1098/rspa.1977.0162.

[52] R.Z. Shakirov, D.A. Topchiev, V.A. Kabanov, L.P. Kalinina, The effect of isobutylamine on the radical polymerization of methacrylic acid in dioxan, Polym. Sci. U.S.S.R. 14 (1) (1972) 42–52, https://doi.org/10.1016/0032-3950(72)90362-0.

[53] E.A. Rafikov, M.D. Gol`dfein, A.D. Stepukhovich, The kinetics of the inhibited methacrylic acid polymerization in bulk and in solution, Polym. Sci. U.S.S.R. 23 (1981) 77–83, https://doi.org/10.1016/0032-3950(81)90298-7.

[54] S. Beuermann, D.A. Paquet, J.H. McMinn, R.A. Hutchinson, Propagation kinetics of methacrylic acid studied by pulsed-laser polymerization, Macromolecules 30 (2) (1997) 194–197, https://doi.org/10.1021/ma9611073.

[55] S. Beuermann, M. Buback, P. Hesse, I. Lacík, Free-radical propagation rate coefficient of nonionized methacrylic acid in aqueous solution from low monomer concentrations to bulk polymerization, Macromolecules 39 (1) (2006) 184–193, https://doi.org/10.1021/ma051954i.

[56] J. Barth, M. Buback, SP-PLP-EPR study into the termination kinetics of methacrylic acid radical polymerization in aqueous solution, Macromolecules 44 (6) (2011) 1292–1297, https://doi.org/10.1021/ma102278n.

[57] M. Schmitt, Introduction to analyzing the solidification of multifunctional acrylic esters by ESR, Analyst 138 (2013) 3758–3770, https://doi.org/10.1039/c3an36869f.